

Oceans and Climate: Circulation and interbasin exchanges in the Southern Ocean.

Wilhelmus P.M. de Ruijter (project leader), Fred H. Walsteijn, and Raymond C.V. Feron

Institute for Marine and Atmospheric Research, Utrecht University
Princetonplein 5, 3584 CC Utrecht, The Netherlands

Introduction

The relatively warm climate of western Europe is strongly related to the Gulf Stream that branches north-westward as the warm North Atlantic Current. Evidence is piling up that in the recent past the climate state changed between warm and cold modes on time scales of decades only (e.g., Boyle and Keigwin [4], Dansgaard et al. [7], Harvey [22]). These are directly related to switches in the global scale thermohaline circulation in the ocean. This study focuses mainly on the Southern Ocean part of the circulation, where major interbasin transports take place. Variations in these exchanges may lead to significant global responses, particularly in the North Atlantic sector (Gordon [18]). Main theme of this project is the study of interbasin and intergyre exchanges in the Southern Ocean by performing sensitivity studies of the Antarctic Circumpolar Current in a numerical model and by determining mesoscale eddy exchanges and the associated mean circulation from satellite altimeter data. Results of both project components are summarized below in subsequent sections of this short paper.

1 The Antarctic Circumpolar Current

The Antarctic Circumpolar Current (ACC) is an essential component of the climate system in that it accomplishes a significant poleward flux of heat and exchanges water masses and properties between the South Atlantic, Pacific, and Indian oceans (see, e.g., Nowlin and Klinck [29]). Therefore, reliable prediction of global climate change requires knowledge of the dynamical balance of this vital component and its sensitivity to changes in external and internal parameters.

Measurements and model studies have provided the following characterization of the dynamical balance of the ACC (Nowlin and Klinck [29], McWilliams et al. [26], Marshall et al. [25]). Momentum input by wind stress is concentrated horizontally into a few narrow circumpolar jets by a high eddy activity in the upper ocean. Zonal momentum is transported downward, to the deep ocean, by isopycnal form stress induced by geostrophic eddies. Momentum is finally removed from the ACC by topographic form stress due to meanders in the deep ocean. Poleward heat transfer is directly related to this downward momentum transfer: if it is assumed that the momentum input is transferred downward completely, then the equivalent heat transport is close to the estimated loss of heat to the atmosphere south of the Polar Front (Marshall et al. [25]).

However, key properties, such as the magnitude and variability of the ACC volume transport, still have not been explained satisfactorily. For example, the dependence of the ACC volume transport on the strength of the windforcing has been predicted by a number of simplified models, but there is no consensus at all. Baker [2] predicts a linear

relation (see also Godfrey [17], Straub [31]), while the concept of Johnson and Bryden [23] yields a transport proportional to the square root of the zonal wind stress. Marshall et al. [25] and Straub [31] give transport estimates that have no direct dependence on the wind stress. In the latter case only density stratification emerges as the dominant factor. As a second example, bottom friction plays no significant role in the momentum balance, but it is the most important energy sink of the system. Therefore, the sensitivity of model results to the value of this parameter has to be established.

1.1 Sensitivity study of the ACC

The present study uses eddy-resolving simulations. Such high resolution is mandatory because transient eddies are a vital link in the ACC dynamics, as described above. The ACC has been modeled as a limited area quasi-geostrophic flow in a channel with schematic continents (Walsteijn [33]), similar to an earlier approach of McWilliams et al. [26]. As external parameters were varied: density stratification and magnitude and meridional structure of the applied zonal wind stress. Internal parameters that were varied are: bottom friction magnitude, position and width of Drake Passage, height and shape of topography, domain size, and type of lateral viscous terms (Laplacian or hyperviscosity). Each parameter was varied for two variants of the lateral viscous boundary conditions: either “no-slip” or “slip” conditions were used.

1.2 Results

When slip boundary conditions are applied, the model ACC shows a vacillation between a blocked state and an unblocked state with westward and eastward transports, respectively (Fig. 1a). Clearly, variability is large in comparison with observed Drake Passage transports. In this case an eastward zonal wind stress has been applied with a sinusoidal structure. The zero of its curl coincides roughly with the northern edge of Drake Passage. A reduction of the wind stress magnitude causes the ACC to become unblocked, i.e., it resides predominantly in the unblocked state. When the wind stress magnitude is increased or bottom friction reduced the flow no longer succeeds in sustaining a prolonged separation from the tip of “South America”. Consequently, it predominantly resides in the blocked state (Walsteijn [33]). This reluctance to separate is a physically unrealistic feature of the case with slip boundary conditions. The blocked and unblocked states themselves are not sensitive to variations in the parameters except the density stratification, in the same way as for the case with no-slip boundary conditions (described below). Interestingly, the model ACC is hardly affected by mild topographic height variations and the width and position of Drake Passage.

When no-slip boundary conditions are used, the model ACC resides persistently in an unblocked state (Fig. 1b). The jet always separates from the south edge of “South America”. The mean ACC transport is insensitive to variations of most of the abovementioned parameters. If the wind stress magnitude is increased or the bottom friction reduced only the amplitude of barotropic fluctuations is enhanced. A reduction of bottom friction by a factor of 16 is sufficient to obtain an energy balance where lateral and bottom friction dissipate energy at equal rates. Reducing bottom friction by a factor of 400 leads to

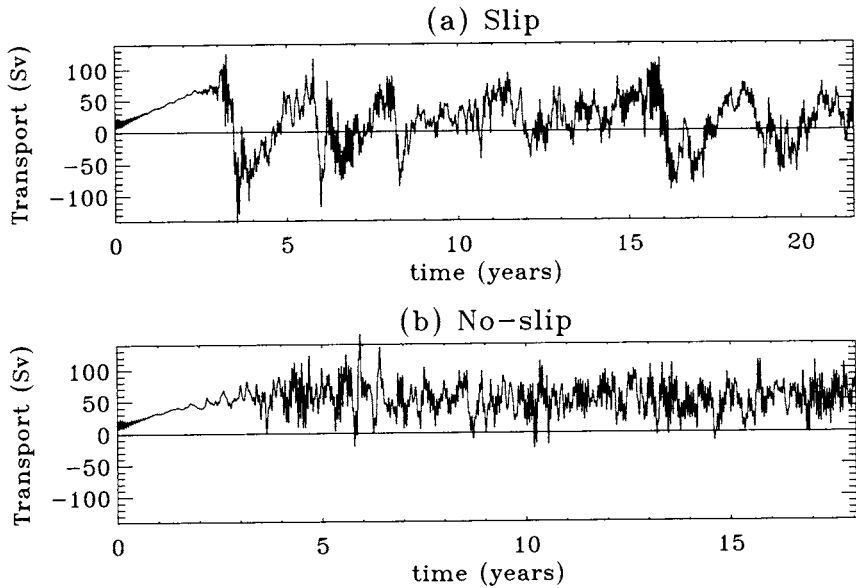


Figure 1: Time series of eastward circumpolar volume transport (in $10^6 \text{ m}^3/\text{s}$) obtained from simulations with two layers and a sinusoidal zonal wind stress. Panel (a): slip boundary conditions; panel (b): no-slip boundary conditions.

a flow in which lateral friction constitutes the dominant energy sink. However, in the momentum and vorticity balances interface stresses and topographic form drag remain dominant (see Walsteijn [33]).

The most important factors that determine the volume transport are stratification and the meridional structure of the wind stress. Reducing the stratification leads to a reduction of the transport almost linearly with the first internal deformation radius (Fig. 2). (See Walsteijn [33] for a discussion.) Shifting the zero-contour of the wind stress curl to the north gives a more realistic position of this line relative to the tip of “South America”. The average meridional position of the ACC coincides with this line, except where the ACC is affected by topography or continents (Fig. 3a). Surprisingly, a northward shift turns out to have no significant effect on the ACC volume transport. If the wind stress curl is zero (i.e., the wind stress is uniform) the ACC mainly follows an alternative “southern” path, dictated by the iso-lines of ambient potential vorticity, although weaker “northern” paths can be distinguished as well (Fig. 3b). The volume transport is increased with respect to cases where a significant wind stress curl determines the ACC’s position entirely (Fig. 2). Also, the sensitivity of the transport to the stratification is larger. In summary, the meridional distribution of wind stress determines the path(s) followed by the ACC. Preferred paths lie along ambient potential vorticity contours and at the latitude where the wind stress curl crosses zero, i.e., at the wind stress maximum. The transport is largest if both paths are fully active, e.g., when the wind stress maximum occurs at a northern latitude while the forcing is still large at southern latitudes (Figs. 3c and 4).

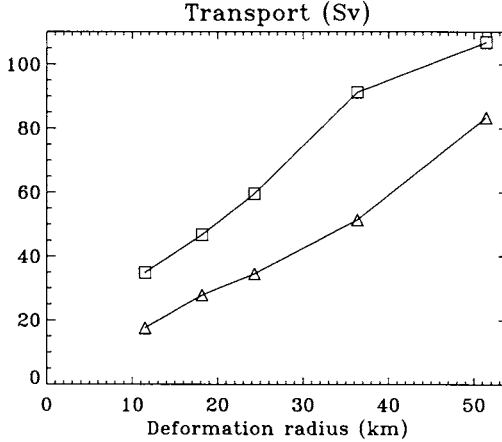


Figure 2: Time-mean circumpolar volume transport as a function of the internal Rossby deformation radius (i.e., the strength of the density stratification), for two-layer flow in a small domain with no-slip boundary conditions. Line \triangle : the zonally directed wind stress has a sinusoidal meridional structure. Line \square : the wind stress is uniform.

2 Eddies and mean flow in the Southern Ocean: analysis of satellite altimeter data

Satellite systems are most effective in providing observations necessary to understand the oceans on a global scale. Observations of the sea surface height can be obtained by a satellite altimeter (e.g. Douglas and Cheney [9], Feron [12]). Sea surface height is directly related to ocean currents and their variations. In this part of the study three years of Geosat-data (GEODetic SATellite) were used from its Exact Repeat Mission (ERM) to determine eddy fluxes and the associated mean circulation in highly energetic regions of the Southern Ocean

One of these areas lies around South Africa where the Agulhas Current system interconnects the warm Indian Ocean with the relatively cold Southern Atlantic (Gordon et al. [19], Lutjeharms et al. [24]). The heat and fresh water fluxes between these two oceans takes place largely by enormous Agulhas rings (with diameters of order 300 km) that pinch-off from the Agulhas Current and penetrate the Atlantic (Boudra and De Ruijter [5], Gordon et al. [19], Wakker et al. [32]).

Part of the Agulhas volume transport leaks directly into the South Atlantic. This leakage of warm Indian Ocean water, which is not well defined, together with the import of Agulhas rings may be a critical link in the global thermohaline ocean circulation and thus also in the climate system (De Ruijter [8], Gordon [18], Broecker [3]).

Although the detection of Agulhas rings in the relatively quiet South Atlantic subtropical gyre is rather straightforward (Gordon and Haxby [20], Naeije et al. [27]), the shedding process is difficult to extract from altimeter measurements. In ocean areas with strong currents, like the Agulhas Current, the inability ¹ to determine the total flow field

¹This inability is caused by the fact that the exact shape of the geoid is unknown (Cheney and Marsh [6], Nerem et al. [28], Rapp and Wang [30]).

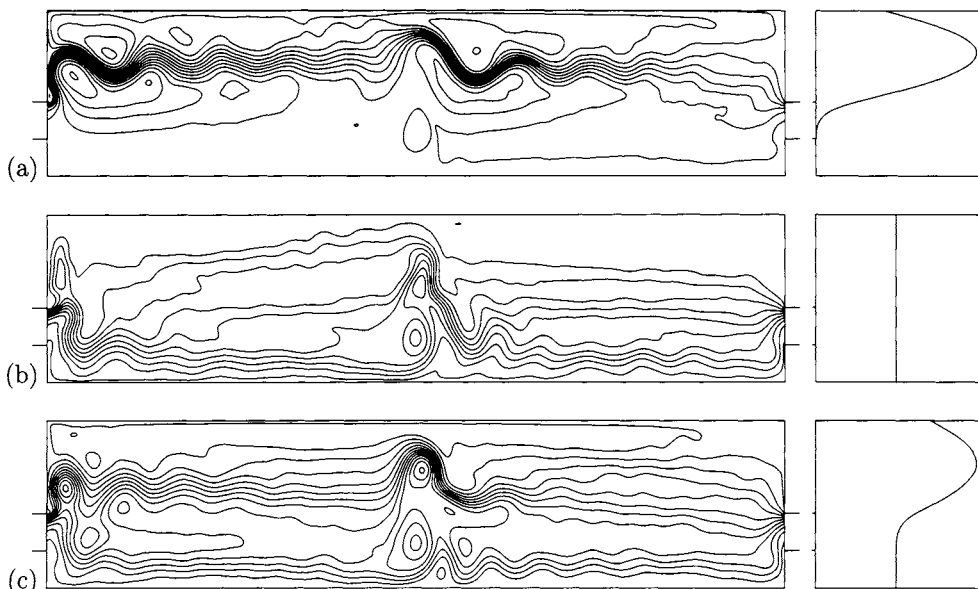


Figure 3: Time-mean upper layer streamfunction (left panels) in a model of the Antarctic Circumpolar Current for three different meridional distributions of the zonally directed wind stress (right panels). In the top row (a) the wind stress has a sinusoidal structure, with a maximum about 400 km north of Drake Passage and a zero plateau at southern latitudes. In the middle row (b) the wind stress is uniform. The lower row (c) gives a case where the wind stress is a mixture of the two other cases. Both “southern” and “northern” paths are now clearly present. No-slip boundary conditions were used, except for slip conditions at the northern domain boundary. Tickmarks indicate edges of Drake Passage, where periodic boundary conditions hold. The model has three layers, and first internal Rossby deformation radius of 24.31 km. Domain size is 6275×1412 km. Bottom topography consists of mounts in Drake Passage and at the center of the domain. Contour interval is 3 Sverdrups (3×10^6 m³/s).

leads to artificial eddy-like structures in the relative satellite altimeter observations. In those ocean regions it is difficult to distinguish between rings and current meanders.

Mesoscale eddies also play a significant role in the meridional exchange between the Antarctic Circumpolar Current (ACC) and the subtropical wind-driven gyres. The area of interaction between the ACC and the subtropical gyres is characterized by thermocline outcropping and has strong frontal features. This is also the area where the thermocline interacts directly with the atmosphere and where the thermal and haline properties of the ocean are established. Quantifying the heat and fresh water exchanges across these confluence fronts should be an essential ingredient of a climate observation system. We are presently at a stage of developing the analysis methods that will lead to such quantifications from satellite observations.

In view of the above the following main goals of this part of the study emerge: 1) to detect mesoscale ring formations and study their subsequent trajectories and evolution from radar altimeter observations without knowing the exact shape of the geoid and 2) to derive the mean surface flow field from satellite altimeter observations of horizontal eddy fluxes.

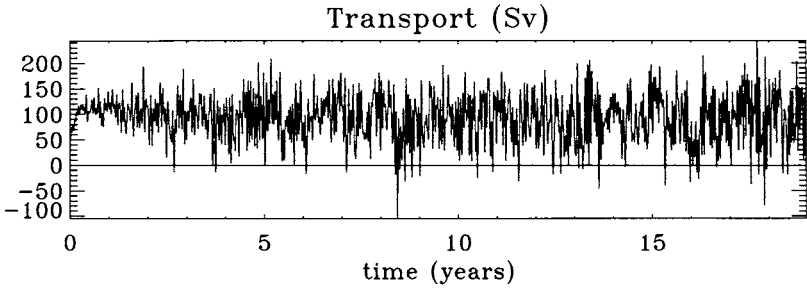


Figure 4: Time series of eastward circumpolar volume transport (in $10^6 \text{ m}^3/\text{s}$) for the case in Fig. 3c.

2.1 Results

Combination of harmonic analysis and principal component analysis enables the extraction of typical Agulhas Current frequencies of the sea surface dynamic topography from the 3-year Geosat altimetric data set. Applying these techniques to successive sea level anomaly maps in the Agulhas retroreflection area indicates that 18 events took place over a 3-year analysis period. Variations occur from year to year. The combined analysis shows that the first three modes (principal components) of variability are statistically dominant. The structure of the spatial and temporal scales leads to the hypothesis that these modes are associated with periodic Agulhas front movements, culminating in the formation of large Agulhas rings. Sharp changes (pulses) in the sea level pattern then determine the time of pinch-off. If these pulses can be connected to the formation of large Agulhas Rings, they are of great importance for the large-scale circulation because the rings contribute significantly to the energy and fresh-water flux between the Indian Ocean and South Atlantic (Feron et al. [11]). The validity of our hypothesis was confirmed by applying the same techniques to the UK, Fine Resolution Antarctic Model (Webb et al. [34], Feron [14]).

As a logical extension the method has been also applied to two other western boundary current systems in the Southern Ocean, the East Australian Current and the Brazil-Malvinas (or Falkland) Confluence, leading to a catalogue of Geosat-observed ring shedding events in both current systems (Feron [13], Feron [14]).

Active research is ongoing, also in our group, to estimate the impact of these eddies on the global meridional fluxes of momentum, heat and fresh water (Drijfhout [10], Feron [16], Van Ballegooyen et al. [1])

In the final part of this project we have developed a method to calculate mean sea surface dynamic topography (MSSDT) and thus the ocean surface circulation from the observed temporal variability (Feron [15]). Averaging of the potential vorticity balance leads to a relation between the mean divergence of the eddy-vorticity fluxes and the time-averaged vorticity field. The former can be derived from the satellite altimeter observations. Our method appears to be applicable to areas of the ocean with sufficiently strong mesoscale variability such as the major western boundary currents and their extensions and to the frontal regions of the Antarctic Circumpolar Current (Feron et al. [15]). Surprisingly realistic results followed for the Southern Ocean (Fig. 5, Feron [15]). An im-

portant application is to combine the newly derived averaged flow field with the observed eddy field to derive the total time-varying surface velocity field. As a striking example this has been applied to the Agulhas Current retroflexion where the repeated shedding of large rings can now be reconstructed as a continuous process (Fig. 6). In principle, our method could form the basis of a monitoring system for such highly energetic areas.

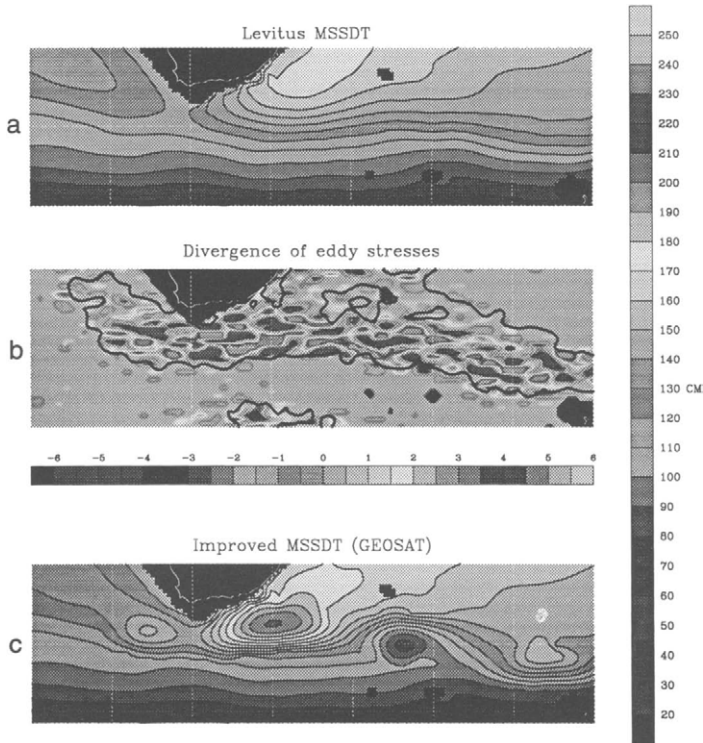


Figure 5: (a) The Mean Sea Surface Dynamic Topography (MSSDT) in the Agulhas Extension in dynamic cm from Levitus, 1982 climatology, relative to 1000 dbar, (b) the mean divergence of the eddy vorticity flux, (units: $\times 10^{-13} s^{-2}$), derived from satellite altimeter observations, (c) improved MSSDT solution (i.e., surface flow field) from our new approach, contour interval is 10 cm.

3 Summary and Conclusions

In the Earth's climate system the redistribution of heat between equatorial and polar regions takes place in approximately equal amounts by the ocean and the atmosphere. Variations in these transports on decadal, and larger, time scales are mainly due to changes in the ocean's thermohaline circulation. In the Southern Ocean cross frontal exchanges, largely by mesoscale eddies, form an essential component of the global meridional overturning circulation of the ocean. Observing and realistically modeling those exchanges and their variability in time should therefore be an integral part of a Global Climate

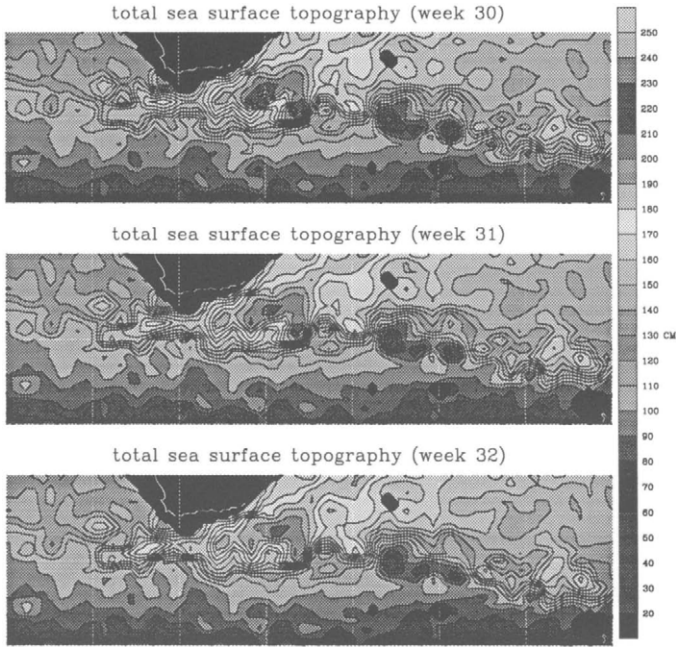


Figure 6: A time sequence of the absolute dynamic height in the Agulhas Retroflexion at weekly intervals determined by applying the method of (Feron et al., 1994) to Geosat altimeter height observations. In this sequence the actual shedding of large Agulhas rings south of Africa can be observed. Analysis of the 3-year observational period shows that 18 similar ring-shedding events occurred. These rings carry a large amount of heat into the South Atlantic, and thus establish one of the interbasin links in the global heat and fresh water circulation. Time is relative to 8 november 1986 and the contour interval is 10 cm.

Observing and Forecasting System. In this project a few fundamental steps have been taken toward developing such a system.

The first part of the present study has revealed the sensitivity of a new eddy-resolving model of the Antarctic Circumpolar Current (ACC) to its external and internal parameters. The ACC is most sensitive to the vertical density stratification and the wind stress profile (Walsteijn [33]). Depending on the wind stress profile the ACC consists of one or more jets. When wind stress has a significant curl, an ACC jet emerges that is forced towards the latitude where the curl crosses zero, i.e., where the wind stress is maximal. An alternative or second jet occurs if the wind stress is large at latitudes south of Drake Passage. Then the volume transport increases significantly as does its sensitivity to the stratification. The time-mean transport of simulations with a large domain and broad wind stress profile (e.g., Fig. 4) is of the same order as the observed value (cf. Nowlin and Klinck [29]). The transport history of the model shows realistic time scales, such as mild modulations with periods on the order of 6 months to several years. However, barotropic fluctuations with a period of roughly 25 days have an amplitude which is about three times larger than corresponding fluctuations in observations. Using a more realistic topography (e.g., by including small-scale “bottom roughness”) would probably reduce the

magnitude of these fluctuations to more realistic levels.

The dynamics of ACC jets are determined by transient eddies and the density stratification. Eddy activity is strongly affected by changes in stratification (Walsteijn [33]). The strength of the reverse feedback is still unknown, i.e., it is unclear to which degree the eddy heat transport is coupled with the stratification and thermohaline overturning. This is an area of active research. A full description of (sensitivities of) the ACC variability and transports requires both eddy-resolution and more complete thermodynamics than is present in a quasi-geostrophic model. For future climate research it is, therefore, important to extend the present sensitivity study to a system of primitive equations.

The possibility to synoptically study the ocean's eddy field and related mean circulation from satellite altimeter observations has been verified and explored in the second part of this study. Progress has been made concerning the generation mechanism, formation rates, trajectories, translation speeds, and lifetime/dissipation rates of eddies in the Southern Ocean western boundary currents. Over the 3 year observational period of Geosat approximately 18 large rings pinched-off from the Agulhas Current, south of Africa. The majority of these rings reaches the South Atlantic. Just after being formed Agulhas rings have the largest translation speed, approximately 8 cm/s . When they move out of the highly active Agulhas retroflection area their translation speed reduces to approximately 4 cm/s . The associated volume transport on a yearly basis is at least $7 \times 10^6 \text{ m}^3/\text{s}$, approximately half of the total exchange between these two oceans. We therefore conclude that Agulhas rings contribute significantly to the Indian-South Atlantic connection and the associated heat and fresh water flux.

Van Ballegooyen et al. [1] estimated from a combined hydrographic-altimeter study that the net heat fluxes (300 Wm^{-2}) and evaporative losses (1 cm/day) to the atmosphere due to eddies within the Agulhas region are appreciable larger than the summer climatological means for this region. Their volume flux $6.3 - 7.3 \times 10^6 \text{ m}^3/\text{s}$ is consistent with other estimates. Similarly, they estimate fluxes of heat and salt into the Atlantic Ocean via the Agulhas eddy field of 0.045 PW and $78 \times 10^{12} \text{ kg}$ per year, respectively.

In the concluding part of this work, which is still ongoing, we try to better determine how the eddy field interacts with and modifies the mean circulation and how it is coupled to the deeper circulation. Coupling with numerical models will lead to improved estimates of meridional and cross frontal fluxes. First results are promising and show that it appears to be possible to improve the estimates of the mean sea surface dynamic topography by using satellite altimeter observations of horizontal eddy momentum and vorticity fluxes (Feron et al. [15]).

Partly due to the success of Geosat, new altimeters are now operational. With the successful European Remote Sensing Satellite (ERS1) and Topex/Poseidon new altimeter data is becoming available with increased absolute accuracy and precision (Haagmans et al. [21]). Aside from major improvements in the new altimeter observations, the continuity of observations and their accurate analysis is a high priority for future climate studies aiming at Global Ocean and Climate Forecasting.

Acknowledgment. This investigation was supported by the Dutch National Research Programme on Global Air Pollution and Climate Change, projectnumber 850025, and the Stichting Ruimte Onderzoek Nederland (SRON). Computations were performed on the CRAY Y-MP and CRAY C90 at the Academic Computing Centre (SARA), Amsterdam, The Netherlands. Use of these supercomputer facilities

was sponsored by the Stichting Nationale Computerfaciliteiten (National Computing Facilities Foundation, NCF), with financial support from the Nederlandse Organisatie voor Wetenschappelijk Onderzoek (Netherlands Organization for Scientific Research, NWO). Delft University of Technology (section for Space Research and Technology and Faculty of Geodesy) is acknowledged for the altimeter data processing.

References

- [1] Ballegooyen, R.C. van, M.L. Gründlingh, and J.R.E. Lutjeharms, *J. of Geophys. Res.*, *99*, 14053–14070, 1994.
- [2] Baker, D.J., Jr., *J. Mar. Res.*, *40*, suppl., 21–26 (1982).
- [3] Broecker, W.S., *Oceanography*, *4*, 79–89, 1991.
- [4] Boyle, E.A. and L.D. Keigwin, *Nature*, *330*, 35–40, 1987.
- [5] Boudra, D.B. and W.P.M. De Ruijter, *Deep Sea Res.*, *33*, 447–482, 1986.
- [6] Cheney, R.E. and J.G. Marsh, *EOS Trans*, AGU 62(45), 743–752, 1981.
- [7] Dansgaard W., J.W.C. White, and S.J. Johnson, *Nature*, *339*, 532–533, 1989.
- [8] De Ruijter, W.P.M., *J. Phys. Oceanogr.*, *12*, 361–373, 1982.
- [9] Douglas, B.C. and R.E. Cheney, *J. of Geophys. Res.*, *95*, 2833–2836, 1990.
- [10] Drijfhout, S.S., PhD thesis, Utrecht University, 1992.
- [11] Feron, R.C.V., W.P.M. De Ruijter, and D. Oskam, *J. Geophys. Res.*, *97*, 9467–9477, 1992.
- [12] Feron, R.C.V., *Change*, *11*, 6–7, 1992.
- [13] Feron, R.C.V., *Satellite Altimetry in Geodesy and Oceanography*, Springer-Verlag, Berlin, 1992.
- [14] Feron, R.C.V., accepted in *J. Geophys. Res.*, 1994.
- [15] Feron, R.C.V., W.P.M. de Ruijter, and P.J. van Leeuwen, Submitted to *J. Geophys. Res.*, 1994.
- [16] Feron, R.C.V., PhD thesis, Utrecht University, 1994.
- [17] Godfrey, J.S., *Geophys. Astrophys. Fluid Dynamics*, *45*, 89–112, 1989.
- [18] Gordon, A.L., *J. Geophys. Res.*, *91*, 5037–5046, 1986.
- [19] Gordon, A.L., J.R.E. Lutjeharms, and M.L. Gründlingh, *Deep Sea Res.*, *34*, 565–599, 1987.
- [20] Gordon, A.L. and W.F. Haxby, *J. Geophys. Res.*, *95*, 3117–3125, 1990.
- [21] Haagmans, H.N., M.C. Naeije, and R.C.V. Feron, *Geodetical Info Magazine*, *5*, Nov-Dec 1993
- [22] Harvey, L.D.D., *Quaternary Science Reviews*, *8*, 137–149, 1989.
- [23] Johnson, G.C. and H.L. Bryden, *Deep-Sea Research*, *36*, 39–53, 1989.
- [24] Lutjeharms, J.R.E., W.P.M. De Ruijter, and R.G. Peterson, *Deep Sea Res.*, *39*, 1791–1807, 1992.
- [25] Marshall, J., D. Olbers, H. Ross, and D. Wolf-Gladrow, *J. Phys. Oceanogr.*, *23*, 465–487, 1993.
- [26] McWilliams, J.C., W.R. Holland, and J.H.S. Chow, *Dyn. Atmos. Oceans*, *2*, 213–291, 1978.
- [27] Naeije, M.C., Wakker K.F., R. Scharroo, and B.A.C. Ambrosius, *ISPRS, J. Photogramm. Rem. Sensing*, *47*, 347–368, 1992.
- [28] Nerem, R.S., B.D. Tapley, and C.K. Shum, *J. Geophys. Res.*, *95*, 3163–3179, 1990.
- [29] Nowlin, W.D., Jr. and J.M. Klinck, *Rev. Geophys. Space Phys.*, *24*, 469–491, 1986.
- [30] Rapp, R.H. and Y.M. Wang, *Geophys. J. Int.*, *117*, 511–528, 1994.
- [31] Straub, D.N., *J. Phys. Oceanogr.*, *23*, 776–782, 1993.
- [32] Wakker, K.F., R.C.A. Zandbergen, M.C. Naeije, and B.A.C. Ambrosius, *J. Geophys. Res.*, *95*, 2991–3006, 1990.
- [33] Walsteijn, F.H., In preparation, 1994.
- [34] Webb, D.J., P.D. Killworth, A.C. Coward, and S.R. Thompson, Natural Environment Research Council, 1991.